

# Melting and crystallization behaviour of elastoplastic semicrystalline copolymers: poly(ether ester)

E. Pedemonte, M. Leva, E. Gattiglia and A. Turturro

Centro Studi Chimico-Fisici di Macromolecole Sintetiche e Naturali, Corso Europa 30,  
16132 Genova, Italy

(Received 21 December 1984)

The melting and crystallization behaviour of an elastoplastic semi-crystalline poly(etherester) has been studied by differential scanning calorimetry. The shape of the melting endotherm is strongly dependent on heating rate and annealing time and results from the sum of simultaneous melting and crystallization phenomena. Samples prepared by different techniques, i.e. by solvent evaporation or by melt extrusion, behave very differently owing to specific crystal morphologies. By applying the Hoffman-Weeks plot, the equilibrium melting temperature has been extrapolated. The Avrami treatment allows the calculation of the index  $n$  and of the rate constant  $K$  from the isothermal kinetic data.

(Keywords: melting; crystallization; annealing; poly(etherester); differential scanning calorimetry; morphology)

## INTRODUCTION

Thermoplastic elastomers are block copolymers, characterized by elastomeric behaviour associated with thermoplasticity, mouldability and dimensional stability, similar to those of linear thermoplastics.

The macrostructure of this class of polymers is multiphase, due to the presence in the molecule of hard and soft segments which are thermodynamically immiscible.

In the solid state, the soft phase imparts to the material elastomeric properties, while the hard phase forms thermally reversible physical crosslinks.

The hard segments can consist either of a glassy amorphous polymer or of a crystallizable sequence such as polystyrene in well known styrene-butadiene-styrene three-block copolymers and polyester in poly(ether esters), respectively.

The class of poly(ether ester)s, and specifically the Hytrel family, seems to be particularly interesting both from theoretical and practical points of view. Hytrels are Du Pont products<sup>1-4</sup> described by the general formula  $(A_n B_m)_z$ :

Hard segment A =  $-\text{CO}-\text{C}_6\text{H}_4-\text{CO}-\text{O}-(\text{CH}_2)_4-\text{O}-$

Soft segment B =  $-\text{CO}-\text{C}_6\text{H}_4-\text{CO}-\text{O}-[(\text{CH}_2)_4-\text{O}]_x-$

The polyether block has a molecular weight of about 1000 ( $x \approx 15$ );  $m$ ,  $n$  can vary over a wide range of values, thus leading to materials with high versatility in terms of final properties, namely hardness, elastic modulus, melting point, etc. Since synthesis in the early 1970s, use of these materials has been growing in several applications. Recently, new practical interest has been shown in the field of polymer blends, as Hytrels seem to have the capability of improving the impact resistance of some important technopolymers such as polyamides.

However, at present these copolymers have not been deeply studied. Most papers, even the recent ones, deal with morphological characterization<sup>5-8</sup>: the macrostruc-

ture, as elucidated by electron microscopy, consists of continuous and interpenetrating crystalline and amorphous phases, the crystallites being dispersed throughout the soft liquid-like matrix. According to Jelinsky *et al.*<sup>9</sup>, <sup>13</sup>C n.m.r. analysis gives evidence of a two phase structure characterized by very low degree of mixing at the domain boundaries. In contrast, the thermal behaviour is rather unknown. Wegner *et al.*<sup>10,11</sup> investigated the influence of the isothermal crystallization kinetics on the morphology and the mechanical properties, pointing out also that the copolymer composition bears little relevance for the supermolecular structure and the related properties.

As a research group involved in polymer blend fields and in toughening of polyamides we are interested to investigate Hytrel's thermal behaviour, studying the pure polymer as well as some blends with other components. Furthermore, this study could give valuable information for the investigation of blends containing one semicrystalline component.

In the present paper, the melting behaviour of a pure Hytrel will be thoroughly investigated and different techniques of specimen preparation will be considered. Some correlations with the morphology will be attempted.

## EXPERIMENTAL

### Materials

Our investigations have been carried out with Hytrel 5556, produced by Du Pont de Nemours in form of pellets. Some characteristics, as reported by the technical sheet, are: specific gravity  $1.20 \text{ g cm}^{-3}$ ; melt index  $7 \text{ g/10 min}$ ; 100% modulus  $13.8 \text{ MPa}$ . The copolymer has been used without further characterization. 2,2,3,4,4,4-Hexafluorobutanol, kindly supplied by Montefluos SpA, was used as solvent.

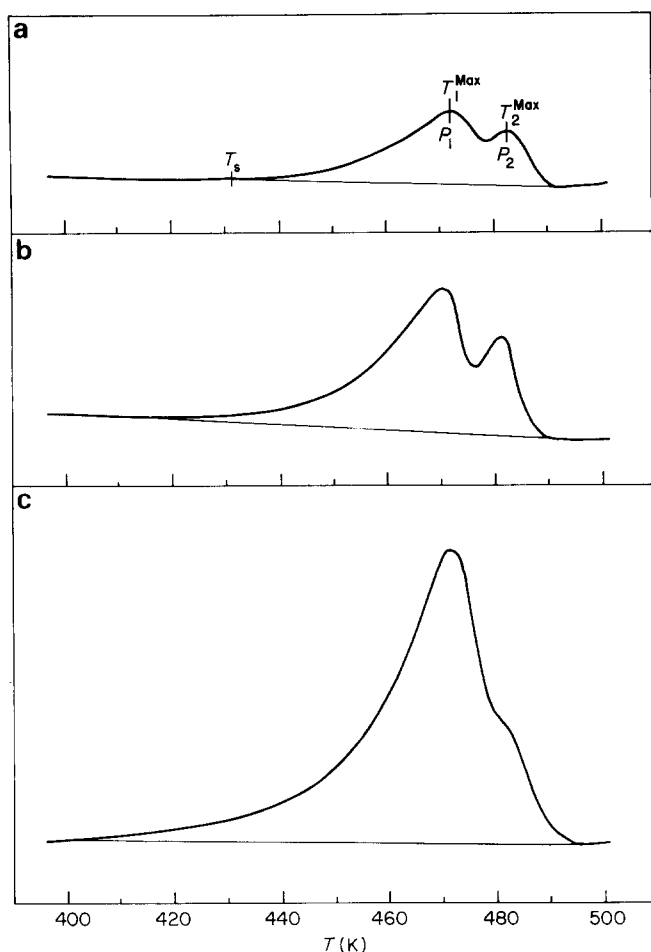


Figure 1 Melting curves of slowly evaporated films scanned at different heating rates. (a)  $20 \text{ K min}^{-1}$ ; (b)  $40 \text{ K min}^{-1}$ ; (c)  $80 \text{ K min}^{-1}$

#### Specimen preparation

Specimens have been prepared by two different methods: isothermal evaporation of dilute solutions and melt extrusion. In the first case two controlled rates were used ( $1$  and  $20 \text{ cm}^3 \text{ h}^{-1}$ ), which from now on will be indicated as slow and fast evaporation rate. Specimens were dried at  $50^\circ\text{C}$  under vacuum for about 1 week (constant weight has been assumed as index of total solvent removal). The melt extrusion was performed at approximately  $T = 275^\circ\text{C}$ ; the apparatus was equipped to obtain thin rods (diameter 1 or 2 mm), some of which have been stretched on line during the cooling (stretching ratio about 2).

#### Techniques and measurements

Morphological observations have been carried out by transmission electron microscopy using a Siemens Elmiskope 102 apparatus. Sections  $600\text{--}1000 \text{ \AA}$  thick have been cut with a diamond knife from embedded specimens, using a Reichert OmU-2 ultramicrotome equipped with a Shandon FC 150 device, which allows us to freeze specimen and blade at  $-110^\circ\text{C}$  and  $-60^\circ\text{C}$  respectively. To improve the staining, sections have been wetted for 15 min with a  $0.2\%$  aqueous solution of phosphotungstic acid.

Thermal scanning and isothermal crystallization have been followed with a Perkin Elmer DSC 2 calorimeter equipped with the model 3500 Data Station. Heating rate

of  $20 \text{ K min}^{-1}$  and cooling rate of  $10 \text{ K min}^{-1}$  have been used, if not differently quoted. The melting behaviour has been investigated at rates ranging between  $5$  and  $80 \text{ K min}^{-1}$ , doing an accurate temperature calibration at every scanning rate; the isothermal crystallizations have been carried out by melting the copolymer at  $540 \text{ K}$  for  $5 \text{ min}$  and rapidly cooling the specimen at the selected temperature.

## RESULTS AND DISCUSSION

### Melting behaviour

In Figure 1 the melting curves of slowly evaporated films scanned at some different heating rates are shown. The following features can be underlined:

- the thermogram is characterized by a double peak curve ( $P_1$  and  $P_2$ );
- the lower temperature peak ( $P_1$ ) becomes more and more relevant on increasing the heating rate;
- the temperature of the maximum ( $P_2$ ) decreases on increasing the heating rate.  $T_1$  does not change monotonically (Table 1);
- the apparent heat of fusion (cal/g of total polymer) changes with the heating rate, as reported in Table 1;
- the deviation of the melting curve from the base line of the thermogram occurs at temperatures  $T_s$  lower and lower as the heating rate increases.

This behaviour finds a reasonable explanation in the frame of the morphological model suggested for this copolymer<sup>5</sup>. It is well known that the hard segments of the macromolecules are supposed to segregate into crystalline regions, which are randomly dispersed inside the amorphous phase, formed by the soft segments. These join together the ordered aggregates, which act as physical crosslinks and can be destroyed by raising the temperature of the specimen above the melting point. It is argued that the crystalline regions are rather small and irregular; the organization of the hard segments inside would correspond to the fringed micelle model rather than to the folded chain lamellae.

It is known that the crystalline regions melt at different temperatures according to their dimensions and degree of internal order<sup>12</sup>. Our experiments show that when the temperature of the specimen is raised very rapidly ( $80 \text{ K min}^{-1}$ ), the endothermal effect starts to be measurable at rather low temperature ( $400 \text{ K}$ ) and covers a large range of values (from  $400$  to  $495 \text{ K}$ ); it points towards the presence of a wide dispersion in crystal size and degree of order. The thermogram is strongly asymmetric and shows one maximum only, together with a shoulder which will be discussed later.

The fast scanning prevents the recrystallization of the undercooled molten polymer so that the thermogram would correspond to the actual morphology of the original specimen. In contrast a slower heating rate

Table 1 Relevant characteristics of melting curves of slowly evaporated films

Heating rate ( $\text{K min}^{-1}$ )	$\Delta H_m$ (cal $\text{g}^{-1}$ )	$T_s$ (K)	$T_1^{\text{max}}$ (K)	$T_2^{\text{max}}$ (K)
5	8.4	—	472.4	484.6
20	14.1	430	472.3	482.4
40	13.0	415	471.0	481.5
80	12.6	400	472.0	481.5

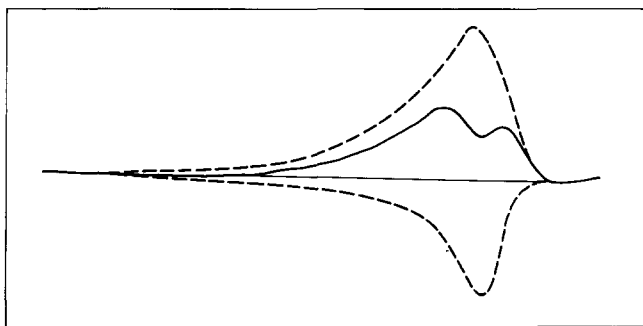


Figure 2 Schematic representation of the exothermic and endothermic contributions which lead to the double peak melting curve (the 20 K min<sup>-1</sup> thermogram of Figure 1)

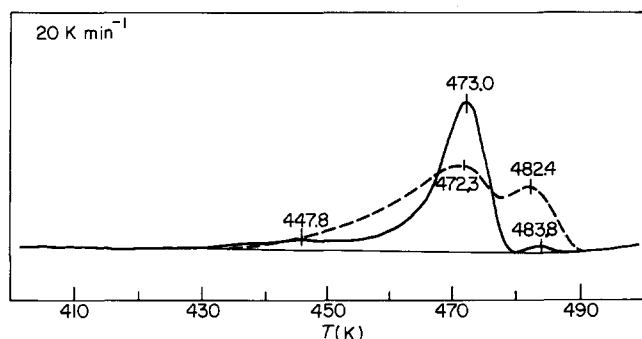


Figure 3 First (---) and second (continuous curve) melting curves of a slowly evaporated film. The molten specimen has been non-isothermally crystallized in the calorimeter by cooling down at 10 K min<sup>-1</sup> from 540 K (5 min) to 340 K

allows the undercooled molten polymer to crystallize again in more regular aggregates and an exothermic effect overlaps the melting phenomenon, as recently discussed by Rim and Runt<sup>13</sup>. It can be argued that its maximum lies between 470 and 480 K; the pattern is strongly asymmetric and ends sharply in the high temperature range. Point (a) gives a reasonable explanation so far as the double peak profile is the consequence of the heat balance between two opposing contributions and does not involve any specific meaning for the maxima (Figure 2).

Points (b) and (e) come from a proper combination of the exothermic and endothermic contributions; it could be correlated both with the actual morphology of the crystalline regions and with the chain mobility of the hard segments, as the recrystallization occurs when the thermal scanning is slower than the reorganization rate. When the heating rate is fast the process is hindered and constrained only in the high temperature range, so that the deviation of the melting curves from the baseline is measurable at lower temperature and  $P_1$  becomes more relevant. The shoulder of the curve obtained at 80 K min<sup>-1</sup> follows a small amount of recrystallization.

Point (c) is the consequence of a complicated combination of the two aforementioned effects and it will not be discussed further.

Finally point (d) can be explained if one takes into account that higher enthalpic contents are associated with more regular ordered regions obtained by recrystallization and crystal perfection<sup>14</sup>. The apparent heat of fusion of the copolymer increases when experiments are carried out with progressively slower heating rate, allowing polymer reorganization to be performed to a larger

extent. At 5 K min<sup>-1</sup> the calorimeter sensibility must be also accounted for; the area effect<sup>15</sup> is significant and is able to explain the low measured values of  $\Delta H_m$ .

Figure 3 shows the thermogram obtained by immediately remelting a specimen which has been non-isothermally crystallized in the calorimeter by cooling from 540 to 340 K. The crystallization process leads to a symmetrical curve which has its maximum at 443.5 K. The second melting curve is different from the original one; it consists of an asymmetric peak (maximum at 473.0 K) together with two very small secondary maxima, at 447.8 and 483.8 K.

In the frame of the model suggested before, this pattern can be explained by considering that the non-isothermal crystallization of the molten copolymer allows the formation of aggregates smaller and less regular than those present in the original film, prepared by slow evaporation of the solvent from a dilute solution. As a matter of fact the deviation of the thermogram from the baseline occurs at lower temperature (410 K) and the whole endothermic effect is reduced (11.4 cal g<sup>-1</sup>). The recrystallization is supposed to be more relevant.

The results reported in Figure 4 give definite support to the model. In these experiments, during the second melting run, the scanning has been stopped at 477.1 K and switched on again after 1 h and 30 min respectively; in such a way the recrystallization can go on isothermally and a large amount of the crystals melt as soon as the temperature is raised: remarkable endothermic effects, which are a function of the annealing time at 477.1 K, are actually measured.

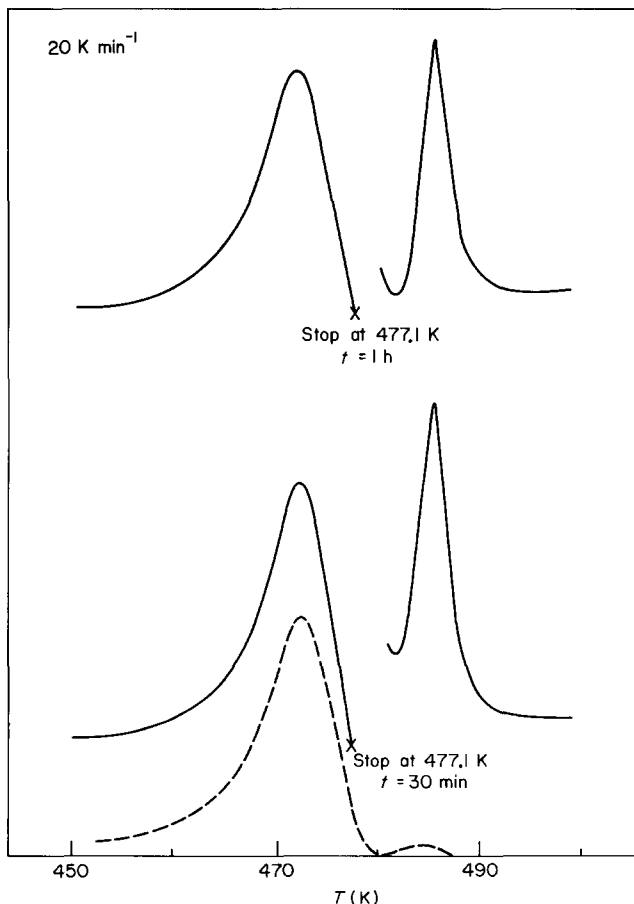
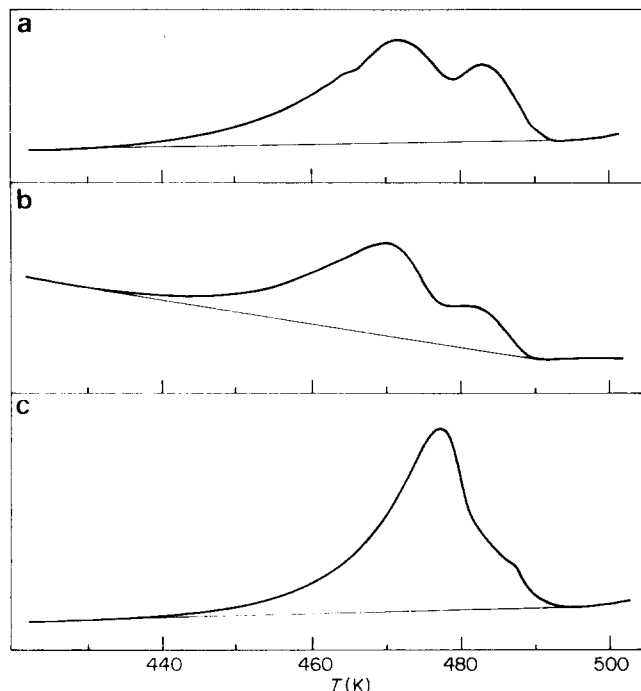


Figure 4 Second melting curve of the specimen of Figure 3. The scanning has been stopped at 477.1 K and switched on again after 1 h and 30 min respectively



**Figure 5** Melting curves of specimens prepared by using different techniques. (a) Slowly evaporated cast film; (b) rapidly evaporated cast film; (c) extruded dia. 2 mm

**Table 2** Characteristics of melting curves of specimens prepared with different techniques

Specimen	$\Delta H_m$ (cal g <sup>-1</sup> )	$T_s$ (K)	$T_1^{\max}$ (K)	$T_2^{\max}$ (K)
Cast films				
Slowly evaporated	14.1	430	472.3	482.4
Rapidly evaporated	6.9	415	469.5	481.0
Extruded rods (dia. 2 mm)	8.9	400	478.1	—
Extruded (dia. 1 mm) and stretched rods	12.0	420	475.3	484.3
Original pellets	10.7	360	474.8	483.8

If one compares the melting curves of specimens prepared with different techniques (Figure 5 and Table 2) it can be argued that cast films slowly evaporated from dilute solutions do have a more regular organization of the crystalline phase. In extruded rods poorly ordered regions are present, whose melting starts to be measurable from 400 K; the recrystallization of the undercooled polymer is so large that a small exothermic effect is registered between 410 and 450 K.

The structural order of the extruded specimens can be improved by reducing their diameter and stretching the filament. At the same time the chain mobility is reduced by orientation: the whole thermal effect does not change remarkably with heating rate, and the melting curves are perfectly smooth in the high temperature range when the polymer is experimented on at 80 K min<sup>-1</sup> (Figure 6).

#### Morphological analysis

The morphologies of several specimens are reported in Figure 7. Apparently no relevant difference exists between slowly and rapidly evaporated cast films where a random distribution of ordered domains inside the rubbery phase is detected; in the latter case the phase separation is coarser and the crystalline regions have smaller dimen-

sions. Some specific patterns can be found in extruded specimens and have to be correlated with the orientation of the structure. Regions of single lamellae, having an average thickness of about 50 Å, are visible, in agreement with previous results of other authors<sup>7,10</sup>.

However morphological analysis seems to be a rather poor technique to identify specimens prepared with different methods; different conclusions have been reached with other block polymers (ABA three-block copolymers<sup>16</sup>, for instance). The explanations have to be found both in the similarity of the chemical nature of the blocks and in the short and irregular dimensions of the block lengths.

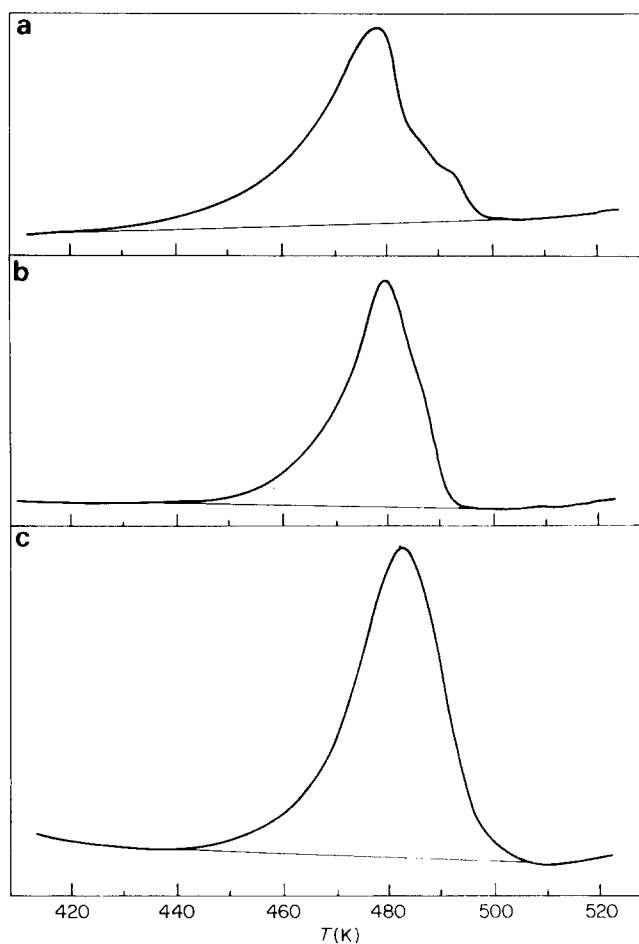


**Figure 6** Melting curves of extruded specimens scanned at different heating rates. (a) 20 K min<sup>-1</sup>; (b) 40 K min<sup>-1</sup>; (c) 80 K min<sup>-1</sup>

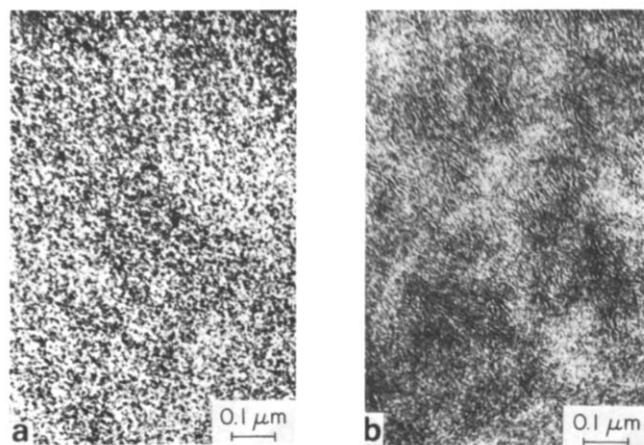


**Figure 7** Electron micrographs of thin sections of (a) a slowly evaporated film and (b) an extruded and stretched filament

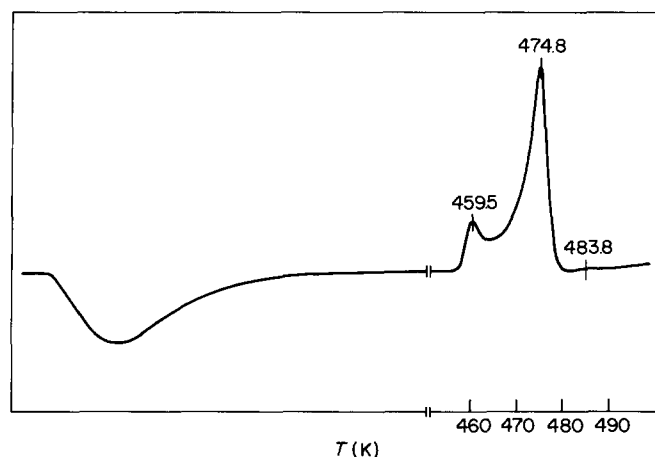


Figure 8 Melting curve of a specimen isothermally crystallized at 453 K in the calorimeter

Table 3 Isothermal crystallization kinetics

$T_c$ (K)	$\Delta H_c$ (cal g <sup>-1</sup> )	$K$	$n$
453	6.2	0.2	2.4
455	4.1	0.12	2.2
459	3.5	0.02	2.1

#### Isothermal crystallization

The melt crystallization of the hard segments inside the amorphous phase generated by the soft ones, has been investigated both from the kinetic and from the thermodynamic points of view<sup>17</sup>. The isothermal crystallization kinetics data have been treated according to the well known Avrami equation<sup>18</sup>. Table 3 collects the calculated values for the overall rate constant  $K$  and the index  $n$ , at the crystallization temperatures  $T_c$ .

Both  $K$  and  $n$  decrease when  $T_c$  increases. The large variation of Avrami constant  $K$  follows the usual trend, as far as the temperature range explored in our experiments is near the melting point. On the other hand the dependence of  $n$  on  $T_c$  is in disagreement with the results of the literature<sup>11</sup>: the explanation can be found if the sensitivity of the calorimeter is considered<sup>15</sup>. The overall thermal effect decreases for experiments at higher temperatures and consequently  $K$  and  $n$  are over- and underestimated respectively.  $K$  would be smaller than 0.2 at 453 K and smaller than 0.02 at 459 K;  $n$  would be larger than calculated and it can be argued that its value is about 3.

#### Equilibrium melting temperature

The thermodynamic equilibrium temperature of perfect crystals into disordered melt,  $T_m^\circ$ , can be evaluated according to Hoffman-Weeks<sup>19</sup> by correlating crystallization and melting temperatures of several specimens.

The melting curve of an isothermally crystallized specimen is shown in Figure 8. It is characterized by an additional peak in the low temperature range, which

corresponds to the actual melting of the isothermally grown crystals; the total area and its position on the temperature scale depends on the annealing time at  $T_c$ . This peak must be considered for the Hoffman-Weeks diagram, since the high temperature peaks represent the final melting of crystals rearranged during the scanning, as discussed previously. In our experiments the annealing time at  $T_c$  has been normalized and the melting curve has been always recorded immediately after the crystallization. It was found that  $T_m^\circ = 515.1$  K.

#### CONCLUSIONS

The main results of our investigation concern the melting behaviour of the etherophasic copoly(ether ester) Hytel 5556. The melting curves present a rather complex feature, correlated with the technique followed in the specimen preparation and with the scanning conditions.

When crystals are grown isothermally from the melt, an endothermic peak is observed a few degrees above the crystallization temperature, which corresponds to the actual melting of the ordered regions. This peak must be considered to build up the Hoffman-Weeks plot, from which  $T_m^\circ = 515.1$  K has been calculated. During the scanning, even at high rate (80 K min<sup>-1</sup>), a continuous reorganization of the structure occurs; it involves endothermic and exothermic effects and leads to more perfect crystals.

The presence of a multipeak pattern in the melting curve of the polymer has been explained taking into account that the exothermic contribution, corresponding to a further crystal perfection, is still present in the melting range. We believe that this behaviour could be rather general and other systems are under investigation.

#### REFERENCES

- Shivers, J. C. US Pat. 3 023 192 (to Du Pont)
- Witsiepe, W. K. US Pat. 3 651 014 (to Du Pont)
- Witsiepe, W. K. US Pat. 3 763 109 (to Du Pont)
- Witsiepe, W. K. US Pat. 3 766 146 (to Du Pont)
- Cella, R. J. *J. Polym. Sci. C* 1973, **42**, 727
- Buck, W. H., Cella, R. J., Gladding, E. K. and Wolfe, J. R. *J. Polym. Sci. C* 1974, **48**, 47
- Seymour, R. W., Overton, J. R. and Corley, L. S. *Macromolecules* 1975, **8**, 331
- Matsuo, M., Geshi, K., Moriyama, A. and Sawatari, C. *Macromolecules* 1982, **15**, 193
- Jelinski, L. W., Schilling, F. C. and Bovey, F. A. *Macromolecules* 1981, **14**, 581
- Zhu, L. L. and Wegner, G. *Makromol. Chem.* 1981, **182**, 3625
- Zhu, L. L., Wegner, G. and Bandara, U. *Makromol. Chem.* 1981, **182**, 3639
- Bassett, D. C. 'Principles of Polymer Morphology', Cambridge University Press, Cambridge, 1981
- Rim, P. B. and Runt, J. P. *Macromolecules* 1983, **16**, 762
- Alfonso, G. C., Pedemonte, E. and Ponzetti, C. *Polymer* 1979, **20**, 104
- Alfonso, G. C., Pedemonte, E., Re, M. and Turturro, A. *Gazz. Chim. It.* 1982, **112**, 99
- Gallot, B. R. M. *Adv. Polym. Sci.* 1978, **29**, 85
- Pedemonte, E., Turturro, A., Dondero, G. and Leva, M. 'Proceedings of XV Congresso Nazionale SCI', Grado, Italy, 1984, p. 312
- Wunderlich, B. 'Macromolecular Physics', Academic Press, New York, 1976, vol. II
- Hoffman, J. and Weeks, J. J. *J. Chem. Phys.* 1962, **37**, 1723